Published in final edited form as:
Biomacromolecules. 2011 January 10; 12(1): 88–96. doi:10.1021/bm101046d.

COMPARATIVE BIODISTRIBUTION OF PAMAM DENDRIMERS AND HPMA COPOLYMERS IN OVARIAN TUMOR-BEARING MICE

S. Sadekar[1,4], **A. Ray**[1,4], **M. Janàt-Amsbury**[3,4], **C. M. Peterson**[3,4], and **H. Ghandehari**[1,2,4,*]

[1]Department of Pharmaceutics and Pharmaceutical Chemistry, Nano Institute of Utah, University of Utah, Salt Lake City, UT 84108, USA

[2]Department of Bioengineering, Nano Institute of Utah, University of Utah, Salt Lake City, UT 84108, USA

[3]Department of Obstetrics and Gynecology, Nano Institute of Utah, University of Utah, Salt Lake City, UT 84108, USA

[4]Department of Center for Nanomedicine, Nano Institute of Utah, University of Utah, Salt Lake City, UT 84108, USA

Abstract

The biodistribution profile of a series of linear *N*-(2-hydroxylpropyl)methacrylamide (HPMA) copolymers were compared with that of branched poly (amido amine) dendrimers containing surface hydroxyl groups (PAMAM-OH) in orthotopic ovarian tumor-bearing mice. Below an average molecular weight (MW) of 29 kDa, the HPMA copolymers were smaller than the PAMAM-OH dendrimers of comparable molecular weight. In addition to molecular weight, hydrodynamic size and polymer architecture affected the biodistribution of these constructs. Biodistribution studies were performed by dosing mice with ^{125}Iodine-labeled polymers and collecting all major organ systems, carcass and excreta at defined time points. Radiolabeled polymers were detected in organ systems by measuring gamma emission of the ^{125}Iodine radiolabel. The hyperbranched PAMAM dendrimer, hydroxyl terminated, generation 5 (G5.0-OH) was retained in the kidney over one week while the linear HPMA copolymer of comparable molecular weight was excreted into the urine and did not show persistent renal accumulation. PAMAM dendrimer, hydroxyl terminated, generation 6.0 (G6.0-OH) was taken up by the liver to a higher extent while the HPMA copolymer of comparable molecular weight was observed to have a plasma exposure three times that of this dendrimer. Tumor accumulation and plasma exposure were correlated with the hydrodynamic sizes of the polymers. PAMAM dendrimer, hydroxyl terminated, generation 7.0 (G7.0-OH) showed extended plasma circulation, enhanced tumor accumulation and prolonged retention with the highest tumor/blood ratio for the polymers under study. Head-to-head comparative study of HPMA copolymers and PAMAM dendrimers can guide the rational design and development of carriers based on these systems for delivery of bioactive and imaging agents.

Keywords

PAMAM dendrimers; *N*-(2-hydroxypropyl)methacrylamide copolymers; enhanced permeability and retention effect; drug delivery; polymer architecture; ovarian tumor

*Corresponding author: hamid.ghandehari@pharm.utah.edu 383 Colorow Road, Salt Lake City, UT 84108 USA.

Introduction

Biocompatible water-soluble polymers have been widely used for a variety of biomedical applications such as drug-delivery and in vivo imaging1. Conjugation of anticancer drugs to polymers has facilitated increased efficacy due to longer circulation half-lives and preferential accumulation in solid tumors due to the enhanced permeability and retention (EPR) effect2. Polymeric prodrugs have also been actively targeted to receptors of malignant cells or endothelial cells of the tumor to increase site-specific localization3¯5. Owing to the stealth properties of water-soluble polymers and their ability to passively and/or actively target solid tumors, polymer therapeutics demonstrate reduced toxicity and higher maximum tolerated doses than small molecular weight anticancer drugs6. Polymeric carriers may be linear such as poly (ethylene glycol) (PEG) and poly(*N*-(2-hydroxypropyl)methacrylamide) (HPMA) or branched such as poly (amido amine) or PAMAM dendrimers (Figure 1).

Copolymers of *N*-(2-hydroxypropyl)methacrylamide (HPMA) with drugs, targeting moieties and imaging modalities have been well characterized for the influence of comonomer structure and composition on solution properties and *in vivo* biodistribution3. Attachment of drugs and targeting moieties alters the random coil conformation of the HPMA homopolymer into a more folded structure, thereby reducing hydrodynamic size, circulation half-live and tumor accumulation7. The charge on the polymer side chains also affects half-life and biodistribution with charged HPMA copolymers being excreted more rapidly than their neutral counterparts8.

Hyperbranched polymers such as PAMAM dendrimers have shown promise as drug carriers for targeted delivery to solid tumors, owing to the nature of synthesis, an extraordinary level of structural control that is achieved for these constructs9, 10. The extent of branching, and nature and number of surface groups have been correlated with toxicity and biodistribution11¯13. Lower generation PAMAM dendrimers have flexible scaffolding, whereas the higher generation systems have a globular, rigid surface14. The lower generation PAMAM dendrimers are excreted through the kidneys whereas the higher generation ones are excreted either by liver alone or by a combination of renal and hepatic routes14. The nature of surface groups influences dendrimer charge, which in turn, is correlated to toxicity both *in vitro* and *in vivo*12, 15¯17. The cationic, amine terminated PAMAMs are more toxic than their anionic or neutral counterparts 12, 15.

Majority of the anticancer water-soluble polymer-drug conjugates in clinical trials have so far been linear in architecture18. The EPR effect, therefore, has been better studied for polymer-drug conjugates with a linear backbone as compared to branched polymeric carriers. Recent work has focused on the influence of polymer architecture on tumor targeting and drug delivery19. A systematic comparison of the effect of polymer architecture on biodistribution, tumor localization, in vivo toxicity and elimination will aid in a rational, pharmacokinetically-guided design of an anticancer drug delivery system. The purpose of this study was to conduct a head to head comparison of the *in vivo* fate of PAMAM dendrimers with linear HPMA copolymers in order to understand the influence of polymer architecture on biodistribution in tumor-bearing mice. This comparison has been done under consistent experimental conditions of polymer characterization and animal model used for biodistribution thus providing valid comparative data of the biodistribution of the two polymer types. The animal model of choice is an orthotopic ovarian tumor model, which is an improvement over widely used xenograft tumor models and better simulates ovarian malignancy. Biodistribution studies were performed by dosing mice with ^{125}Iodine-labeled PAMAM dendrimers and HPMA copolymers of comparable molecular weights. All major organ systems, carcass and excreta were collected at defined time points. Radiolabeled

polymers were detected in organ systems by measuring gamma emission of the ^{125}Iodine radiolabel.

Attachment of drugs, imaging probes and ligands to polymeric carriers is known to affect size, shape and physicochemical properties of the carrier and this would introduce a separate variable in a head to head comparison study. The influence of architecture on drug loading, drug release, cellular delivery and pharmacological activity *in vitro* has been investigated previously. In this study, we have evaluated the influence of polymer architecture on *in vivo* fate in orthotopic tumor-bearing mouse models. To the best of our knowledge, this is the first report attempting to compare the biodistribution of PAMAM dendrimers and HPMA copolymers *in vivo.* The study has implications in rational choice of polymeric carriers for drug delivery.

Materials

Poly (amido amine) dendrimers , hydroxyl-terminated PAMAM-OH generations 5.0, 6.0 and 7.0 were purchased from Sigma Aldrich (St. Louis, MO, USA). N-Succinimidyl-3-(4-hydroxy-3-[^{125}I] iodophenyl) propionate (^{125}Iodine labeled Bolton Hunter reagent) and radioactive sodium iodide (Na^{125}I) were purchased from American Radiolabeled Chemicals (St. Louis, MO, USA). 6-8 weeks old Nu/Nu mice were purchased from Charles River Laboratories (Wilmington, MA, USA). A2780 was procured from American Type Culture Collection (Manassas, Virginia). HPMA homopolymer standards were a gift from Dr. Jindrich Kopecek's laboratory at the University of Utah.

Methods

Polymer synthesis and fractionation

HPMA-copolymer-tyrosinamide-glycylglycyl-ethanolamine poly(HPMA-(GG-EtOH)-(Tyr)) was synthesized and fractionated to obtain weight average molecular weights of 26 and 52 kDa in order to have comparable molecular weights with PAMAM dendrimers, hydroxyl terminated, generation 5.0 (G5.0-OH) and generation 6.0 (G6.0-OH) (Table 1). The HPMA copolymers were synthesized with 20 mole percent glycine-glycine-ethanolamine in order to provide a linear polymer backbone with pendant groups, that facilitate drug loading mimicking previously studied polymers4,20. The side chains were terminated in hydroxyl groups, similar to the terminal groups of PAMAM-OH dendrimers under study to minimize the influence of the chemical nature of side chains and terminal groups on biodistribution.

The comonomers 2-hydroxy(propylmethacrylamide) (HPMA), *N*-methacryloyl-glycyl-glycyl-para-nitrophenyl ester (MA-GG-ONp), *N*-methacryloyl tyrosine-methylester (MA-Tyr) and *N*-methacryloyl-glycyl-glycyl-ethanolamine (MA-GG-EtOH) were synthesized by previously reported procedures21. To synthesize the lower molecular weight HPMA copolymer poly(HPMA-(GG-ONp)-(Tyr)), the comonomers HPMA (78 mole %), MA-GG-ONp (20 mole %) and MA-Tyr (2 mole %) were copolymerized by free radical precipitation copolymerization with azobisisobutyronitrile (AIBN) as the initiator at 50°C for 24 hours using acetone with 10 percent dimethyl sulfoxide as the solvent (Table 1). The copolymer was reacted with ethanolamine to yield hydroxyl-terminated side chains (Figure 2). To synthesize the higher molecular weight HPMA copolymers, poly(HPMA-(GG-EtOH)-(Tyr)), the comonomers HPMA (78 mole %), MA-GG-EtOH (20 mole %) and MA-Tyr (2 mole %) were copolymerized by free radical precipitation copolymerization with AIBN as the initiator at 50°C for 24 hours using acetone-dimethyl sulfoxide as solvent (Table 1, Figure 2). Polymerization was carried out using 12.5 weight % total monomer, 0.6 weight % AIBN and 86.9 weight % solvent. The solvent system used for polymerization was 90% (v/

v) acetone and 10% (v/v) DMSO. The synthesized HPMA copolymers and PAMAM dendrimer, hydroxyl terminated, generation 7.0 (G7.0-OH) (Sigma Aldrich, St. Louis, MO) were fractionated by Size Exclusion Chromatography (SEC) using a Fast Protein Liquid Chromatography (FPLC) system with a Hiload 16/60 Superdex™ preparatory grade column and an ultraviolet detector (GE Healthcare, Piscataway, NJ). PAMAM G5.0-OH and G6.0-OH eluted as monodisperse peaks in a size exclusion chromatograph and did not need to be fractionated. The mobile phase for fractionation was 20% (v/v) acetonitrile and 80% (v/v) phosphate buffer saline (137 mM NaCl, 2.7 mM KCl, 10 mM Na_2HPO_4, 1.76 mM KH_2PO_4, pH 7.4) at a flow rate of 0.5 mL/minute. Eluted peaks were detected at a wavelength of 280 nm.

Polymer characterization

The chromatographic elution profiles of all the HPMA copolymers and PAMAM-OH dendrimers under study were obtained using a Fast Protein Liquid Chromatography (FPLC) system with Superose 6™ 10/300 GL column (GE Healthcare, Piscataway, NJ) and an ultraviolet detector (GE Healthcare, Piscataway, NJ) in order to evaluate relative elution volumes and to check for the absence of small molecular weight impurities. The mobile phase for elution was 20% (v/v) acetonitrile and 80% (v/v) phosphate buffer saline (137 mM NaCl, 2.7 mM KCl, 10 mM Na_2HPO_4, 1.76 mM KH_2PO_4, pH 7.4) at a flow rate of 1.0 mL/minute. Eluted peaks were detected at a wavelength of 280 nm. The molecular weight and molecular weight distribution profile of the fractionated HPMA copolymers were estimated on the same FPLC setup using HPMA homopolymer standards of known molecular weights. The HPMA copolymers, HPMA homopolymer standards and PAMAM-OH dendrimers were further characterized for hydrodynamic radius (R_h) using a Dynamic Light Scattering (DLS) detector (Helleos II) attached to the FPLC system and analyzed using Astra™ 5.3.4.13 software (Wyatt Technologies, Santa Barbara, CA). The tyrosine content in the HPMA copolymers was analyzed by amino acid analysis (University of Utah Core Facility). The zeta potential of polymers dispersed in distilled (DI) water at a concentration of 5.0 mg/ml was measured using a Malvern Instruments Zetasizer Nano ZS (Westborough, MA).

Radiolabeling of polymers

The fractionated HPMA copolymers, containing tyrosine methyl ester in the side chains, were reacted with $Na^{125}I$ (American Radiolabeled Chemicals, St. Louis, MO) at room temperature in phosphate buffer (pH7.4, 0.02M) for 30 minutes with intermittent shaking. 10 mg of HPMA copolymer was reacted with 2 millicurie (mCi) of $Na^{125}I$, dissolved in 0.5 mL of buffer each making up a reaction volume of 1.0 mL. PAMAM dendrimers were reacted with 2200 Ci/mmol of ^{125}Iodine-labeled Bolton Hunter reagent (American Radiolabeled Chemicals, St. Louis, MO) over ice in Borate Buffer (pH 8.5, 0.05M) for 30 minutes with intermittent shaking13. 10 mg of PAMAM dendrimer was reacted with 1 mCi of ^{125}Iodine labeled Bolton Hunter reagent, dissolved in 0.5 mL of buffer each reaching a reaction volume of 1.0 mL. The radiolabeled polymers were dialyzed using clear cellulose ester FloatALyzer® tubes with a cutoff of 3.5 to 5.0 kDa (Spectrum® Laboratories Inc., Houston, TX) against five-4 Liter changes of deionised water over a period of 5 days (one water change per day). Upon dialysis, they were checked for absence of free iodine using a PD-10 size exclusion chromatography column (GE Healthcare, Piscataway, NJ) before use (See Figures 1 and 2 in supporting information). Following dialysis of the reaction volume, the HPMA copolymers showed a specific radioactivity of 1.35 microcurie/mg and the PAMAM dendrimers exhibited radioactivity of 4.5 microcurie/mg of polymer, as measured by a Gamma counter (Cobra Autogamma, Perkin Elmer, Wellesley, MA).

Animal model and tumor inoculation

6-8 week old female Nude/Nude (Nu/Nu) mice were orthotopically inoculated by injecting a cell suspension of 1×10^6 A2780 cells in 10μL of phosphate buffer saline directly beneath the left ovarian bursa22 for all the study groups except PAMAM G7.0-OH. Animals used to assess the biodistribution of G7.0-OH were inoculated with 2×10^5 A2780 cells. The tumor sizes at the time of animal sacrifice and organ harvesting were in the same range as those obtained by inoculation of 1×10^6 cells for other groups. The non-metastatic tumors were allowed to grow for 4 weeks. Tumor size was monitored by palpating the tumors and by change in animal weight. All animal experiments were performed in accordance with the University of Utah IACUC guidelines under approved protocols.

Biodistribution

Five groups of tumor-bearing mice were dosed intravenously by tail vein injection with 50 mg/Kg of radiolabeled G5.0-OH, HPMA copolymer (26 kDa), 40 mg/Kg of HPMA copolymer (52 kDa) and 20 mg/Kg of PAMAM G6.0-OH, and G7.0-OH in 0.2 mL sterile saline. The solution of radiolabeled polymers was mixed with accurately weighed non-radiolabeled polymers in saline to prepare a radioactive dose of about 50,000 cpm per animal. The amount of polymer contributed by the radiolabeled polymer solution in preparing the dose was considered negligible. The mice were sacrificed at defined time points of 5 min, 30 min, 2 hr, 6 hr, 24 hr and 1 wk. All major organ systems were collected including blood, heart, lung, liver, spleen, kidney, tumor, contralateral ovary, brain and the rest of the carcass that included skin, muscle and intestines. Urine and stool were collected by housing animals in metabolic cages and were pooled for all the animals for a given study group at a particular time point. Blood and homogenized carcass were sampled whereas the rest of the organs collected were measured as a whole for radioactive count using a Gamma counter (Cobra Autogamma, Perkin Elmer, Wellesley, MA). All animal experiments were performed in accordance with the University of Utah IACUC guidelines under approved protocols.

In vivo data analysis

The radioactive readings obtained for the individual organs were expressed as a percentage of injected dose normalized to weight of the organ. Statistical Analysis was done using Analysis of Variance (Graphpad Prism®, version 5.01). Area under the curve for plasma time profile was determined by modeling the data on Winnonlin version 2.1 using non-compartmental analysis.

Results and Discussion

Characteristics of the polymers

The PAMAM-OH dendrimers under study were generations 5.0, 6.0 and 7.0 with hydroxyl surface groups. These generations were chosen such that their molecular weights (29, 58 and 117 kDa) lie in the physiologically relevant range for kidney filtration, extended plasma circulation and tumor retention. The two HPMA copolymers synthesized (26 and 52 kDa) were fractionated in order to have comparable molecular weights with PAMAM G5.0-OH and G6.0-OH. The HPMA copolymers were synthesized with 20 mole percent glycine-glycine-ethanolamine side chains in order to provide the linear polymer backbone with pendant groups that typically facilitate the attachment of bioactive and imaging agents4, 20. The polymeric side chains terminated in hydroxyl groups, similar to the terminal groups of PAMAM-OH dendrimers under study in order to minimize the influence of surface or pendant functional group characteristics on comparative biodistribution.

Both the PAMAM-OH dendrimers and HPMA copolymers eluted in the order of decreasing molecular weight within the same polymer series. Comparing the elution times of HPMA copolymers and PAMAM-OH dendrimers of comparable molecular weights, the HPMA copolymer of 52 kDa eluted slightly before the PAMAM dendrimer G6.0-OH (58 kDa) (Figure 3). The hydrodynamic radius of the HPMA copolymer of 52 kDa was also higher than that of PAMAM G6.0-OH (Table 2) as determined by dynamic light scattering. However, in case of the lower molecular weight HPMA copolymer of 26 kDa, an opposite trend was observed with this copolymer eluting after the PAMAM dendrimer G5.0-OH (Figure 3). The hydrodynamic radius obtained by dynamic light scattering was also consistent with the observed trend, with a radius of 1.4 nm for the HPMA copolymer and 2.3 nm for PAMAM G5.0-OH (Table 2). This can be attributed to the difference in architecture of linear HPMA copolymers that have a random coil conformation compared to hyperbranched PAMAM dendrimers which are more compact.

Depending on the chemical nature of the pendant side chains, linear polymers may possess a random-coil architecture in case of hydrophilic groups, an extended chain conformation for negatively charged moieties or a unimicellar folded structure in the case of hydrophobic side groups3. The conformation of hyperbranched polymers such as PAMAM depends on generation with the smaller dendrimers having a flexible scaffolding and higher generations assuming a more compact, globular shape with a dense exterior and relatively hollow interior14. The increment in size of polymers with increase in molecular weight is greater for HPMA homopolymer standards as compared to PAMAM-OH dendrimers (Figure 4). However, below a molecular weight of about 29 kDa, the HPMA copolymers were smaller than the PAMAM-OH dendrimers of comparable molecular weight (Figure 4). Above this molecular weight threshold of 29 kDa, the opposite trend was seen with the random coil HPMA homopolymer standards being larger in hydrodynamic size than the compact PAMAM-OH dendrimers (Figure 4).

The hydrodynamic sizes of amine-terminated dendrimers measured by dilute solution viscometry, light scattering, diffusion nuclear magnetic resonance and theoretically calculated by computer simulations that have been widely reported in literature are slightly higher than the hydrodynamic sizes measured for hydroxyl-terminated dendrimers of the same generation (Table 1)23-25. This can be attributed to a more extended structure of the amine-terminated PAMAMs with charged surface groups as compared to neutral terminal groups in case of the hydroxyl terminated PAMAMs.

Upon comparing the sizes of the HPMA copolymers containing 20 mole % glycine-glycine ethanolamine and 2% tyrosine methyl ester with HPMA homopolymer standards containing 1 % pendant tyrosine groups, the HPMA copolymer of 26 kDa had a hydrodynamic radius of 1.4 nm, comparable to that of the HPMA homopolymer standard (22 kDa). The HPMA copolymer of 52 kDa, however, had a hydrodynamic radius of 3.3 nm, smaller than that of the HPMA homopolymer standard (51 kDa) with a hydrodynamic radius of 4.2 nm. This can be attributed to a higher tyrosine content in the HPMA copolymer of 52 kDa (0.22 mmol tyrosine/g polymer), as measured by amino acid analysis; than the theoretical tyrosine content in the HPMA homopolymer (0.07 mmol/g polymer) (Table 1). An increased number of tyrosine grafts on the HPMA copolymer backbone can lead to intra-molecular, hydrophobic interactions leading to a decrease in the hydrodynamic radius of the HPMA copolymer (52 kDa). Similarly, literature reported values of hydrodynamic radii of HPMA copolymers of similar molecular weights also vary depending on nature and percentage of side chains7.

In vivo biodistribution

The smallest of the PAMAM dendrimers under study, G5.0-OH showed predominant and persistent accumulation in the kidney compared to all other organs (Figure 5A). G6.0-OH was taken up both by the kidney and the liver (Figure 5B). The extent and time of kidney accumulation was much less than G5.0-OH. However, it did not demonstrate extended circulation in the plasma and was taken up by the reticuloendothelial system (RES), thereby accumulating in the liver and spleen. G7.0-OH is known to have a rigid sphere like conformation14. It had a hydrodynamic radius of 4.0 nm and showed the highest plasma circulation time (Figure 5C). This polymer was distributed over all organ systems due to retention in the plasma. Tumor accumulation profile was characteristic of macromolecules with slow accumulation that peaked at 6 hours and retained for 1 week. Small changes in hydrodynamic size of macromolecules in the nanometer range have been known to drastically affect pharmacokinetics26, 27. MRI contrast agents based on PAMAM cores have shown a similar trend when increase in generation affected biodistribution, extravasation and mode of excretion26, 27. PAMAM based gadolinium contrast agents have shown that constructs below 6.0 nm were predominantly excreted via the kidneys, while larger constructs were taken up by the liver instead26. Those constructs in the size range of 5 to 8.0 nm were observed to extravasate into the tumor tissue from tumor vasculature. However, this data had limitations in quantitative interpretation owing to the detection technique (magnetic resonance). The size and conformation of the native PAMAM dendrimers of different generations may have also caused its interaction with plasma proteins, platelets and other components in the blood to differ. Detailed studies on interactions of these native PAMAM dendrimers with blood components could help better explain the effect of size and generation regarding its *in vivo* fate.

HPMA copolymer of 26 kDa with the smallest hydrodynamic radius (1.4 nm) amongst the polymers tested, was excreted through the kidney (Figure 6A) within 2 hours of administration and recovered in the urine (12% of injected dose, see Table 2 in supporting information). It showed slight kidney accumulation (20 % injected dose/g) with slow renal clearance for up to 1 week (6 % injected dose/g). A neutral HPMA copolymer with 5 mol% GFLG-OH and 0.6 mol% tyrosine in the side chains has been reported to have a similar biodistribution profile in a tumor-bearing rat model8. All major organ systems at 1 week were measured to have less than 1 % of injected dose/g including the kidneys8. The difference in kidney accumulation between the reported HPMA-GFLG-OH copolymer and the HPMA copolymer under study can be attributed to the electronegative charge on the HPMA copolymer under study (zeta potential of -15.0mV, Table 2). Reports in literature have demonstrated that anionized linear polymers accumulate in kidneys as a function of electronegative charge28, 29. The HPMA copolymer of 52 kDa circulated in the plasma slightly longer than HPMA copolymer of 26 kDa and showed distribution in all organ systems (Figure 6B). It showed slight tumor accumulation that peaked at 6 hours but did not show prolonged retention at 24 hours. The tumor accumulation of the 52 kDa HPMA copolymer under study seemed less than that reported for HPMA homopolymer of similar molecular weight studied in a tumor-bearing rat model8. The HPMA copolymer under study was seen to be eliminated through urinary excretion with 16 % of the injected dose in the urine 24 hours post injection (see Table 2 in supporting information) and showed negligible liver accumulation. This can be explained due to the difference in hydrodynamic radius of the HPMA copolymer under study and the HPMA homopolymer standard as discussed in the polymer characterization section, thereby highlighting the importance of hydrodynamic size of the polymer in deciding the *in vivo* fate.

The filtration size cut-off for the kidney is known to range from a hydrodynamic diameter of 3.7 to 6.0 nm30. PAMAM G5.0-OH and HPMA copolymer of 26 kDa (<5.0 nm in hydrodynamic diameter) can be readily filtered through the glomeruli. We observed kidney

retention for G5.0-OH for 1 week up to 150 percent injected dose/gram of tissue (Figure 7). However, HPMA copolymer of comparable molecular weight did not persist in the kidney for a week indicating that polymer conformation affected renal reabsorption and retention. Data in literature reports 80 percent of injected dose of PAMAM dendrimer, amine terminated, generation 4.0 (G4.0-NH_2)/gram of kidney tissue, which reduced to about 10 percent of injected dose/gram of kidney upon PEGylating the dendrimer31. It has been reported that PAMAM G4.0-gadollinium complexes accumulate in the proximal straight tubules in the outer medulla stripe of the kidney32. Limited mechanistic studies for renal retention of PAMAM dendrimers report the localization of these polymers in the lysosomes of proximal tubule cells32. This uptake is only possible upon filtration of the dendrimers, providing access to reabsorbtion into the proximal tubules. The biodistribution of acetylated PAMAM G5.0 has been reported in literature and the construct has shown negligible kidney accumulation33. Acetylation may increase the hydrodynamic size of the PAMAM beyond the glomerular filtration cutoff (> 5.0 nm) thereby denying access to proximal tubule cells for uptake. PAMAM G6.0-OH (R_h = 3.0 nm, Table 2) and G7.0-OH (R_h = 4.0 nm, Table 2) studied here are not readily filtered due to their hydrodynamic sizes being above the filtration threshold cutoff and hence do not show prolonged renal retention (Figure 7). The renal uptake for PAMAM G7.0-OH is comparable to that of pegylated G4.0-NH_2 dendrimers reported in the literature31. This indicates that it is possible to reduce non-specific kidney uptake by increasing dendrimer generation to a hydrodynamic size beyond kidney filtration pore size cut-off. The smaller generation G5.0-OH that is observed to accumulate in the kidney may be used for kidney imaging to detect renal tubular damage32, 34. The constructs suggested for this application have been dendrimer-based-magnetic resonance imaging (MRI) contrast agents that are amine terminated32, 34. A hydroxyl-terminated dendrimer such as PAMAM G5.0-OH shows the same or higher extent of kidney accumulation and is likely to be less toxic *in vivo* than the amine terminated dendrimer of same generation11. Inspite of persistent kidney accumulation, PAMAM G5.0-OH did not show elevated kidney toxicity markers at 1 week (refer to supporting information, Figure 3A). An elevated white blood cell count was observed (refer to supporting information, Figure 3B). It has been observed that physicochemically modified HPMA copolymers accumulate in the kidney to a higher extent than their non-modified counterparts8. The introduction of peptide moieties was found to increase kidney accumulation and a direct correlation was observed between the amount of carboxyl and hydrazide groups on the HPMA copolymer and the extent of kidney localization35. HPMA copolymers functionalized with the targeting peptide RGDfK and DTPA (1,2-diamine-N,N-N′,N′,N″,N″-pentaacetic acid) chelating moiety in the side chains showed persistent kidney accumulation that correlated with the amount of peptide loading28. It would be interesting to study the effect of surface modification of PAMAM dendrimers with peptides on kidney accumulation and establish a systematic correlation of the same in non-linear, hyperbranched polymers.

PAMAM dendrimers (G5.0-OH and G6.0-OH) accumulated to a larger extent in the liver than HPMA copolymers of similar molecular weight (26 kDa and 52 kDa) (Figure 8). PAMAM G6.0-OH, with a hydrodynamic radius of 3.0 nm (Table 1) is on the threshold of kidney filtration size cutoff. Hence, its elimination is predominantly by the reticuloendothelial system (RES), with a high extent of accumulation observed in the liver (Figure 8). PAMAM G7.0-OH with its rigid sphere-like globular structure and a hydrodynamic radius of 4.0 nm circulates longer in the plasma than PAMAM G6.0-OH (Figure 8). Its liver accumulation is less than G6.0-OH at the time points under study. However, there is a possibility of an increase in RES organ uptake when the polymer may be eliminated from the tumor (beyond the range of the time points under study). It has been shown that amine terminated PAMAM Generation 4.0 and 5.0 interact with plasma proteins such as human serum albumin, bovine serum albumin and enzymes such as human

erythrocyte acetyl cholinesterase and alter the protein conformation and enzyme activity36¯40. It has also been shown that in the case of other nanoparticulate constructs, smaller particles with higher surface curvature had a better retention of the native protein structure and function than larger nanoparticles41. There is, therefore, a possibility that PAMAM G6.0-OH with a smaller hydrodynamic radius than G7.0-OH and a less dense surface exterior may interact differently with opsonizing proteins, causing it to be taken up by the liver. It would be necessary to investigate how the interaction of the PAMAM dendrimer with opsonizing proteins affects macrophage uptake and consequently *in vivo* fate. Accumulation of PAMAM G6.0-OH up to 40% dose/gram of liver tissue did not affect liver function as indicative of plasma levels of alanine aminotransferase and aspartate aminotransferase (data not shown).

Tumor accumulation profiles are reflective of relative sizes as indirectly measured by size exclusion chromatography with the largest polymer PAMAM G7.0-OH (R_h = 4.0 nm) showing the highest and most persistent tumor accumulation of about 4-6 percent injected dose/gram of tumor tissue up to a week (Figure 9). As is characteristic of the enhanced permeability and retention effect, PAMAM G7.0-OH showed time-dependent accumulation in the tumor that peaked at 6 hours and persisted for up to 1 week with a tumor to blood ratio (T/B ratio) of about 12.7542, 43. The extent of tumor accumulation of HPMA copolymer of 52 kDa was less than the HPMA homopolymer of comparable molecular weight reported in the literature8. This can be attributed to intramolecular interactions amongst tyrosine-containing side chains (0.22 mmol/g of polymer) on the HPMA copolymer leading to a decrease in hydrodynamic radius (3.3 nm, Table 2) as compared to 4.2 nm for the HPMA homopolymer standards. PAMAM G5.0-OH and HPMA copolymer of 26 kDa were cleared from circulation by kidney filtration and hence did not show tumor accumulation. The tumor accumulation data indicated a hydrodynamic radius cutoff of about 4.0 nm, below which prolonged tumor retention was not observed for the orthotopic ovarian carcinoma tumors under study. The HPMA copolymer of 52 kDa with a radius of 3.3 nm showed enhanced tumor accumulation up to 2 % injected dose/gram of tumor. However, it did not show enhanced retention. PAMAM G6.0-OH with a hydrodynamic radius of 3.0 nm did not passively target the tumor (Figure 9).

The plasma exposure of the polymers is consistent with the size exclusion profiles and hydrodynamic sizes of the macromolecules under study (Figure 10A). The largest carrier G7.0-OH (R_h = 4.0 nm) showed the highest plasma exposure, approximately 25 times that of the smaller polymers G5.0-OH and HPMA copolymer of 26 kDa (Figure 10B). The extended circulation time of the PAMAM G7.0-OH allowed enhanced tumor accumulation. Comparing the linear and branched polymers of similar molecular weights, HPMA copolymer of 52 kDa achieved a plasma exposure three times that of PAMAM G6.0-OH (58 kDa) (Figure 10B). This can be attributed to a slightly higher hydrodynamic radius of the HPMA copolymer (R_h = 3.3 nm) as compared to the compact dendrimer (R_h = 3.0 nm) that reduces kidney filtration. PAMAM G6.0-OH was also extensively taken up by the liver (Figure 8), thus reducing its plasma circulation time.

The biodistribution results of the polymeric constructs under study have implications in the choice of carriers for drug delivery and imaging. Due to its selective and persistent kidney accumulation, PAMAM G5.0-OH should be used with caution to deliver drugs such as cisplatinum, methotrexate, stroptozotocin and mitomycin that cause kidney toxicity, but these polymers may be effectively used for kidney imaging to detect renal tubular damage and assess kidney function32, 34. These polymers also have the potential to treat kidney diseases due to preferential renal targeting, which is an area of growing interest. PAMAM dendrimers accumulated in the liver to a higher extent than the HPMA copolymers under study and hence should be used with caution to deliver drugs like adriamycin, methotrexate,

6-mercaptopurine, carboplatin, L-asparaginase and pentostatin that can cause liver damage. High generation PAMAM G7.0-OH showed reduced non-specific uptake in the liver and kidney comparable to that of PEGylated dendrimers31.

The effect of polymer architecture on drug loading, drug release, cellular delivery and pharmacological activity have been evaluated *in vitro*44, 45. In this study, we have evaluated the influence of polymer architecture on *in vivo* fate utilizing orthotopic A2780 ovarian tumor-bearing nude mouse models. Polymer architecture affected renal and hepatic uptake of the constructs under study. The branched PAMAM dendrimers accumulated to a larger extent in the liver than the linear HPMA copolymers. For polymers that could be easily filtered through the kidney, PAMAM dendrimers persisted for a longer period of time in the kidney tissue as compared to HPMA copolymers. This is indicative of a difference in the extravasation of polymers of varying architecture through fenestrations of healthy tissue46. More work is needed to understand the effect of linear and hyperbranched polymer architecture on rates and extent of microvascular extravasation.

Conclusion

Macromolecular architecture affected the increment in hydrodynamic radius of the polymer with increase in molecular weight. Along with molecular weight, polymer architecture and hydrodynamic volume were critical to the *in vivo* fate of the macromolecules. Specifically, polymer architecture affected renal and hepatic uptake of the constructs under study, with the hyperbranched PAMAM dendrimers showing more persistent accumulation than their linear HPMA copolymer counterparts. The difference in hepatic and renal accumulation between PAMAM dendrimers and HPMA copolymers is indicative of a difference in the extravasation of polymers of varying architecture through fenestrations of healthy tissue. Additional studies are needed to understand the effect of the linear and hyperbranched polymer architecture on rates and extent of microvascular extravasation. Tumor accumulation and plasma exposure were correlated with the hydrodynamic size of the polymers. The tumor accumulation data indicated a hydrodynamic radius cutoff of about 4.0 nm, below which prolonged tumor retention was not observed for orthotopic ovarian carcinoma tumors under study. The biodistribution result of the polymeric constructs guides the choice of a carrier of certain architecture and hydrodynamic size for preferential organ accumulation, which can be exploited for drug delivery and imaging applications.

Supplementary Material

Refer to Web version on PubMed Central for supplementary material.

Acknowledgments

We would like to acknowledge Dr. Jindrich Kopecek and Dr. Pavla Kopecekova for providing HPMA homopolymer standards; Yong En Sun, Arnida and Erin Soisson for assistance with animal surgery and organ harvesting; and Daniel B Pike for aiding with the HPMA copolymer synthesis. Financial support was provided by a Catalyst Grant from the University of Utah Health Science Center, NIH grants EB07470, EB007171, DE019050 and the Utah Science Technology and Research (USTAR) initiative.

References

1. Duncan R. Nat. Rev. Drug Discovery. 2003; 2(5):347–360.
2. Fang J, Nakamura H, Maeda H. Adv. Drug Delivery Rev. 2010 DOI:10.1016/j.addr.2010.04.009.
3. Kopecek J, Kopeckova P. Adv. Drug Delivery Rev. 2010; 62(2):122–149.
4. Pike DB, Ghandehari H. Adv. Drug Delivery Rev. 2010; 62(2):167–183.
5. Ulbrich K, Subr V. Adv. Drug Delivery Rev. 2010; 62(2):150–166.

6. Duncan R. Nat. Rev. Cancer. 2006; 6(9):688–701. [PubMed: 16900224]
7. Konak C, Rathi RC, Kopeckova P, Kopecek J. Polymer. 1993; 34(22):4767–4773.
8. Lammers T, Kühnlein R, Kissel M, Subr V, Etrych T, Pola R, Pechar M, Ulbrich K, Storm G, Huber P. J. Controlled Release. 2005; 110(1):103–118.
9. Svenson S, Tomalia DA. Adv. Drug Delivery Rev. 2005; 57(15):2106–2129.
10. Tomalia DA, Fréchet JMJ. J. Polym. Sci., Part A. 2002; 40(16):2719–2728.
11. Duncan R, Izzo L. Adv. Drug Delivery Rev. 2005; 57(15):2215–2237.
12. Kitchens KM, El-Sayed MEH, Ghandehari H. Adv. Drug Delivery Rev. 2005; 57(15):2163–2176.
13. Malik N, Wiwattanapatapee R, Klopsch R, Lorenz K, Frey H, Weener JW, Meijer EW, Paulus W, Duncan R. J. Controlled Release. 2000; 65(1-2):133–148.
14. Tomalia D, Reyna L, Svenson S. Biochem. Soc. Trans. 2007; 35:61–67. [PubMed: 17233602]
15. Jevprasesphant R, Penny J, Jalal R, Attwood D, McKeown NB, D'Emanuele A. Int. J. Pharm. 2003; 252(1-2):263–266. [PubMed: 12550802]
16. Roberts JC, Bhalgat MK, Zera RT. J. Biomed. Mater. Res., Part A. 1996; 30(1):53–65.
17. Sweet DM, Kolhatkar RB, Ray A, Swaan P, Ghandehari H. J. Controlled Release. 2009; 138(1): 78–85.
18. Vicent MJ, Duncan R. Trends Biotechnol. 2006; 24(1):39–47. [PubMed: 16307811]
19. Fox ME, Szoka FC, Frechet JMJ. Acc. Chem. Res. 2009; 42(8):1141–1151. [PubMed: 19555070]
20. Kopecek J, Kopecková P, Minko T, Lu ZR. Eur. J.Pharm. Biopharm. 2000; 50(1):61–81. [PubMed: 10840193]
21. Strohalm J, Kopecek J. Angew.Makromol.Chem. 1978; 70:109–118.
22. Greenaway J, Moorehead R, Shaw P, Petrik J. Gynecol. Oncol. 2008; 108(2):385–394. [PubMed: 18036641]
23. Fritzinger B, Scheler U. Macromol. Chem. Phys. 2005; 206(13):1288–1291.
24. Tande B, Wagner N, Mackay M, Hawker C, Jeong M. Macromolecules. 2001; 34(24):8580–8585.
25. Uppuluri S, Keinath S, Tomalia D, Dvornic P. Macromolecules. 1998; 31(14):4498–4510.
26. Kobayashi H, Brechbiel M. Adv. Drug Delivery Rev. 2005; 57(15):2271–2286.
27. Venditto V, Regino C, Brechbiel M. Mol. Pharm. 2005; 2(4):302–311. [PubMed: 16053333]
28. Borgman M, Coleman T, Kolhatkar R, Geyser-Stoops S, Line B, Ghandehari H. J. Controlled Release. 2008; 132(3):193–199.
29. Kodaira H, Tsutsumi Y, Yoshioka Y, Kamada H, Kaneda Y, Yamamoto Y, Tsunoda S, Okamoto T, Mukai Y, Shibata H. Biomaterials. 2004; 25(18):4309–4315. [PubMed: 15046921]
30. Rippe C, Asgeirsson D, Venturoli D, Rippe A, Rippe B. Kidney Int. 2006; 69(8):1326–1332. [PubMed: 16395274]
31. Kojima C, Regino C, Umeda Y, Kobayashi H, Kono K. Int. J .Pharm. 2010; 383(1-2):293–296. [PubMed: 19761822]
32. Kobayashi H, Kawamoto S, Jo SK, Sato N, Saga T, Hiraga A, Konishi J, Hu S, Togashi K, Brechbiel MW. Kidney Int. 200261(6):1980–1985.
33. Kukowska-Latallo J, Candido K, Cao Z, Nigavekar S, Majoros I, Thomas T, Balogh L, Khan M, Baker J. Cancer Res. 2005; 65(12):5317. [PubMed: 15958579]
34. Dear JW, Kobayashi H, Brechbiel MW, Star RA. Nephron Clin. Pract. 2006; 103(2):c45–c49. [PubMed: 16543755]
35. Lammers T, Subr V, Ulbrich K, Hennink W, Storm G, Kiessling F. Nano Today. 2010; 5(3):197–212.
36. Gabellieri E, Strambini GB, Shcharbin D, Klajnert B, Bryszewska M. Biochim. Biophys. Acta, Proteins Proteomics. 2006; 1764(11):1750–1756.
37. Klajnert B, Bryszewska M. Bioelectrochemistry. 2002; 55(1-2):33–35. [PubMed: 11786335]
38. Klajnert B, Sadowska M, Bryszewska M. Bioelectrochemistry. 2004; 65(1):23–26. [PubMed: 15522688]
39. Klajnert B, Stanisawska L, Bryszewska M, Paecz B. Biochim. Biophys. Acta, Proteins Proteomics. 2003; 1648(1-2):115–126.

40. Shcharbin D, Klajnert B, Mazhul V, Bryszewska MJ. Fluoresc. 2005; 15(1):21–28.
41. Lundqvist M, Sethson I, Jonsson BH. Langmuir. 2004; 20(24):10639–10647. [PubMed: 15544396]
42. Jun YJ, Kim JI, Jun MJ, Sohn YS. J.Inorg Biochem. 2005; 99(8):1593–1601. [PubMed: 15963570]
43. Maeda H, Fang J, Inutsuka T, Kitamoto Y. Int. Immunopharmacol. 2003; 3(3):319–328. [PubMed: 12639809]
44. Khandare J, Jayant S, Singh A, Chandna P, Wang Y, Vorsa N, Minko T. Bioconjugate Chem. 2006; 17(6):1464–1472.
45. Perumal O, Khandare J, Kolhe P, Kannan S, Lieh-Lai M, Kannan R. Bioconjugate Chem. 2009; 20(5):842–846.
46. El-Sayed M, Kiani MF, Naimark MD, Hikal AH, Ghandehari H. Pharm Res. 2001; 18(1):23–28. [PubMed: 11336349]
47. Tomalia DA, Baker H, Dewald J, Hall M, Kallos G, Martin S, Roeck J, Ryder J, Smith P. Polym. J. 1985; 17(1):117–132.

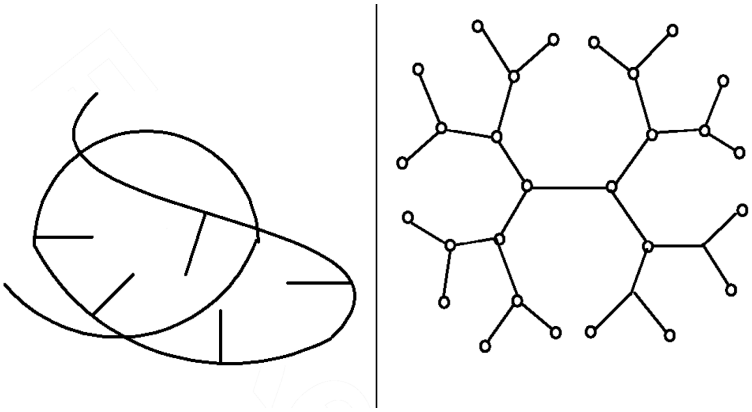

Figure 1.
Schematics of linear random coil HPMA copolymer with side chains (left) and branched PAMAM dendrimer (right).

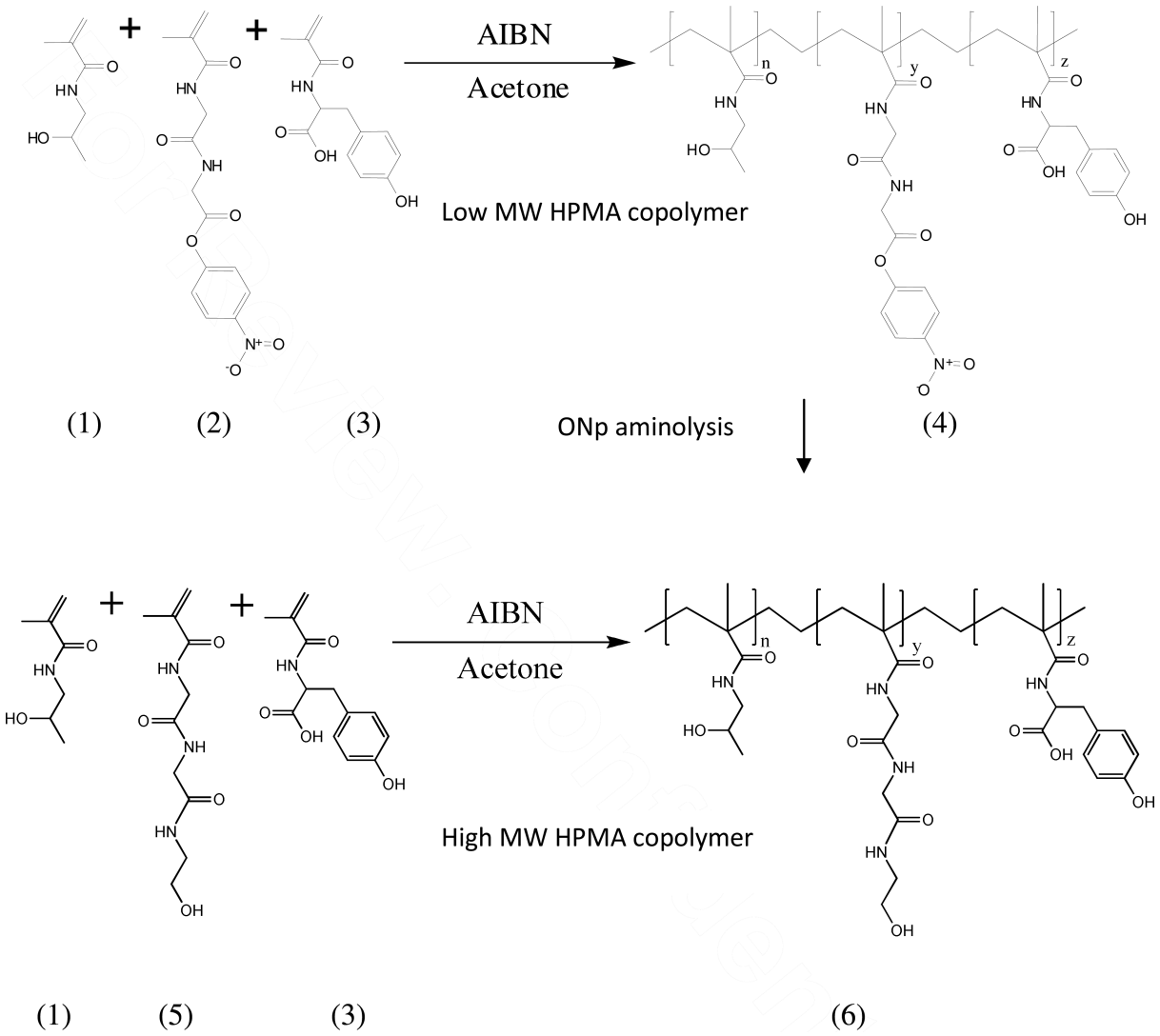

Figure 2.

Synthetic scheme of HPMA copolymers; Copolymerization of the comonomers of HPMA (1), MA-GG-ONp (2) and MA-Tyr (3) by free radical precipitation copolymerization with azobisisobutyronitrile (AIBN) as the initiator to form low MW HPMA copolymer poly(HPMA-(GG-ONp)-(Tyr)) (4) (Feed composition in Table 1); ONP aminolysis of (4) with ethanolamine to form low MW poly(HPMA-(GG-EtOH)-(Tyr)) (6); Copolymerization of the comonomers HPMA (1), MA-GG-EtOH (5) and MA-Tyr (3) by free radical precipitation copolymerization with azobisisobutyronitrile (AIBN) as the initiator to form high molecular weight HPMA copolymer poly(HPMA-(GG-EtOH)-(Tyr)) (6) (Feed composition in Table 1).

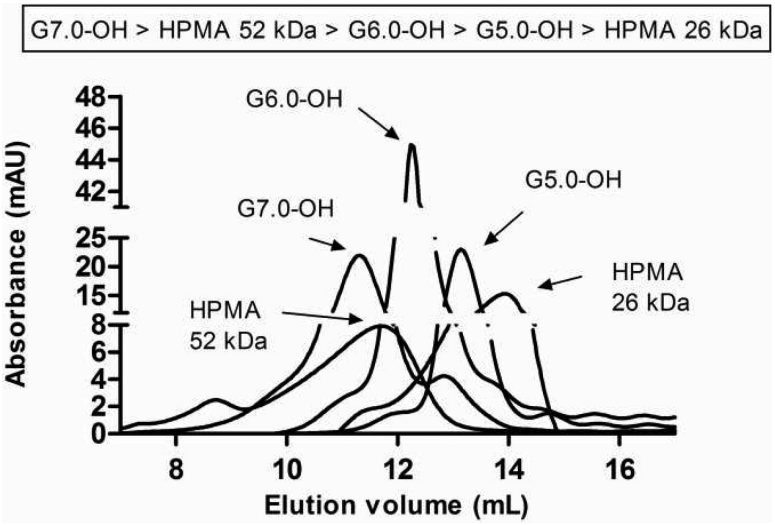

Figure 3.

Size exclusion chromatograms of PAMAM dendrimers and HPMA copolymers using a Fast Protein Liquid Chromatography (FPLC) system with Superose 6™ 10/300 GL column (GE Healthcare, Piscataway, NJ) and an ultraviolet detector (GE Healthcare, Piscataway, NJ).

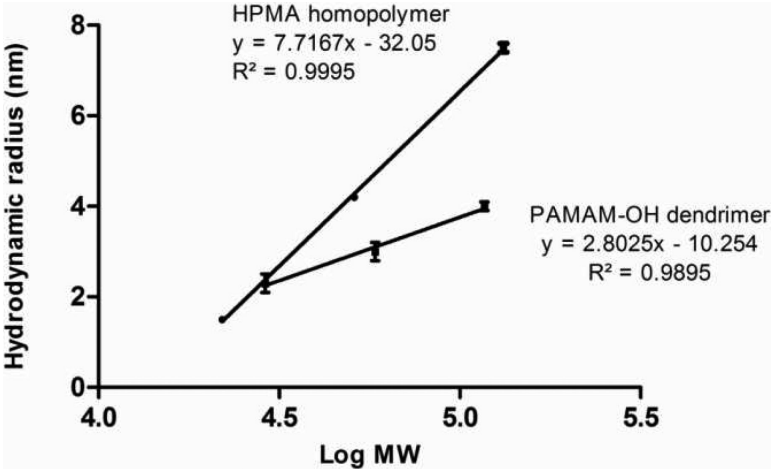

Figure 4.
Correlation of molecular weight with hydrodynamic size of HPMA homopolymer standards and PAMAM dendrimers; Values are mean +/- S.D.; n=3.

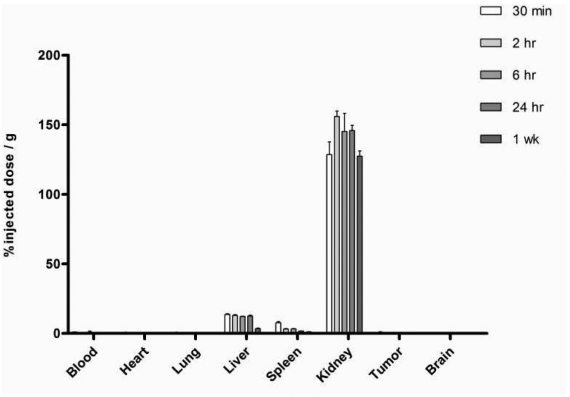

A

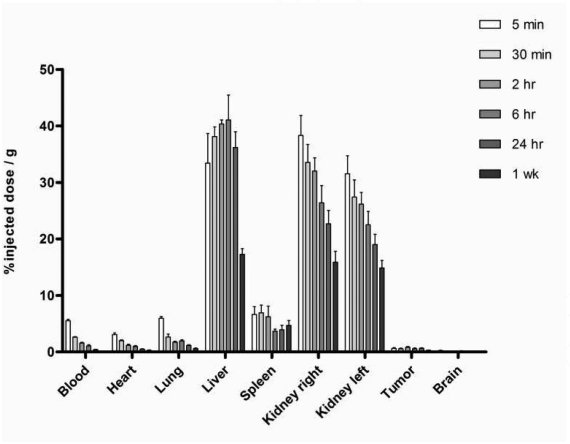

B

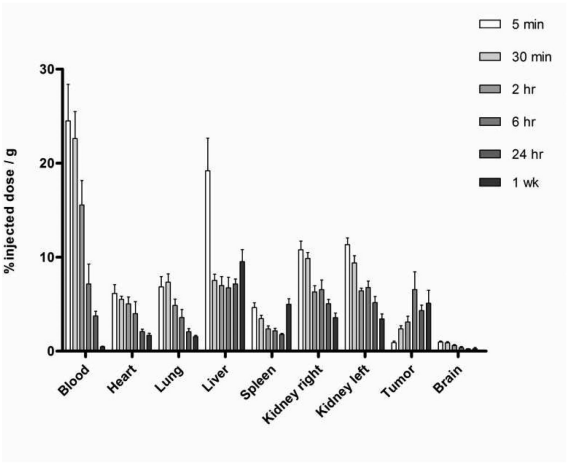

C

Figure 5.

Percentage of injected dose / g of tissue for G5.0-OH (Figure 5A, Top), G6.0-OH (Figure 5B, Middle) and G7.0-OH (Figure 5C, Bottom) in principal organs; Values are Mean +/- SEM; n=5; except n=4 for 5 min 2 hr G5.0-OH; 6 hour and 24 hr G7.0-OH.

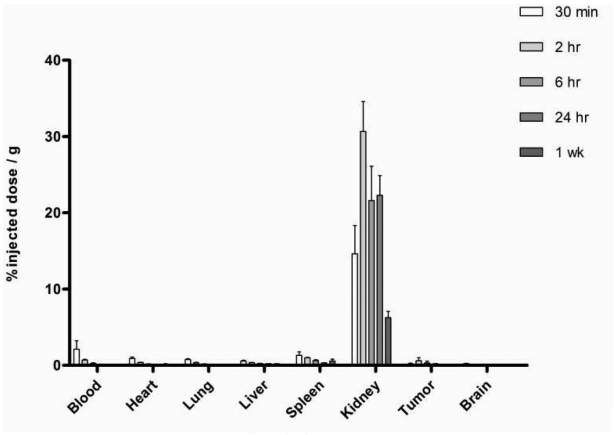

A

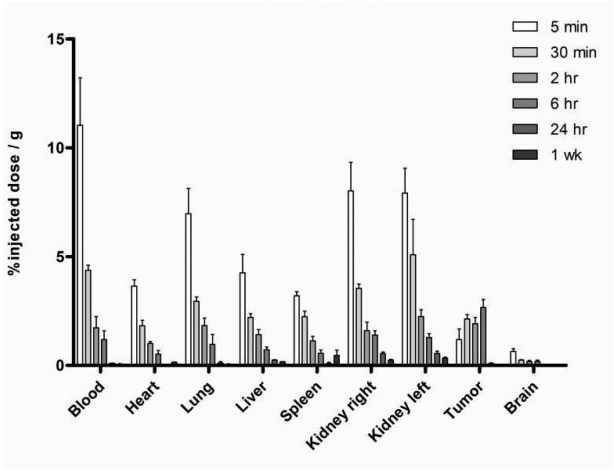

B

Figure 6.

Percentage of injected dose / g of tissue for HPMA copolymer, 26 kDa (Figure 6A, Top) and HPMA copolymer, 52 kDa (Figure 6B, Bottom) in principal organs; Values are Mean +/- SEM; n=5; except n=4 for 5 min HPMA copolymer (52 kDa) and 2 hr HPMA copolymer (26 kDa) and n=3 for 1 wk HPMA copolymer (52 kDa).

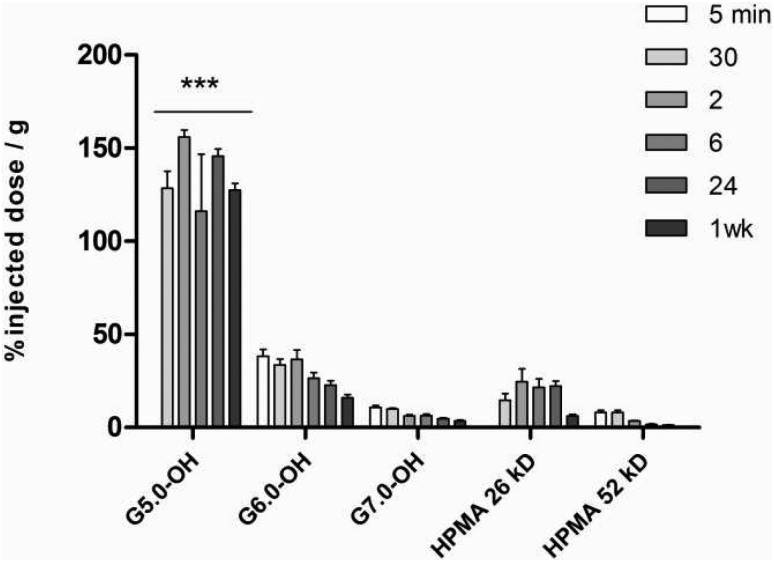

Figure 7.

Percentage of injected dose / g of kidney tissue for PAMAM dendrimers and HPMA copolymers; Values are Mean +/- SEM, n=5; except n=4 for 5 min HPMA copolymer (52 kDa), 2 hr HPMA copolymer (26 kDa) and G5.0-OH; 6 hr and 24 hr G7.0-OH and n=3 for 1 wk HPMA copolymer (52 kDa). *** indicates a statistically significant difference, $p < 0.001$.

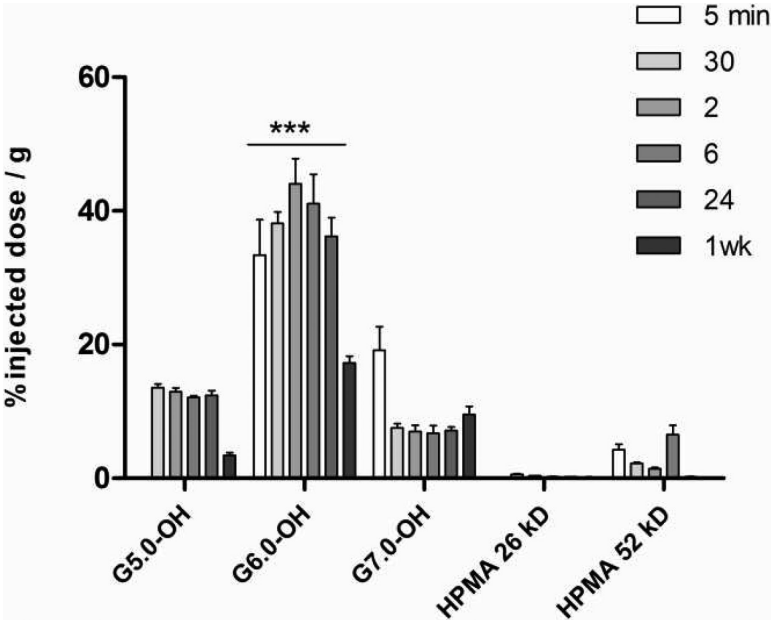

Figure 8.

Percentage of injected dose / g of liver tissue for PAMAM dendrimers and HPMA copolymers, Values are Mean +/- SEM; n=5; except n=4 for 5 min HPMA copolymer (52 kDa), 2 hr HPMA copolymer (26 kDa) and G5.0-OH; 6 hr and 24 hr G7.0-OH and n=3 for 1 wk HPMA copolymer (52 kDa). *** indicates a statistically significant difference, $p < 0.001$.

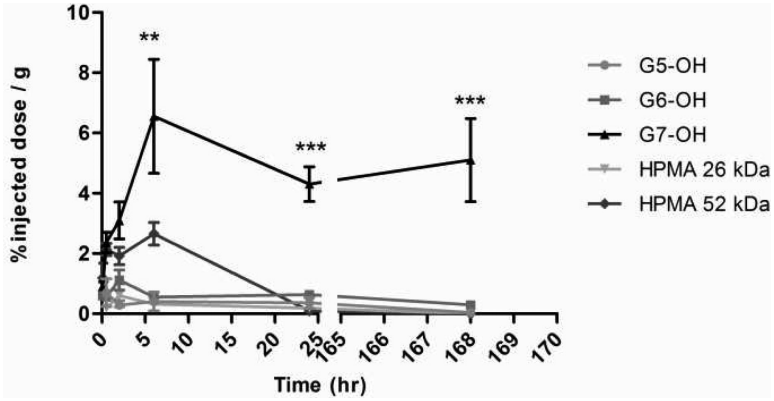

Figure 9.

Percentage of injected dose / g of tumor tissue for PAMAM dendrimers and HPMA copolymers; Values are Mean +/- SEM; n=5; except n=4 for 5 min HPMA copolymer (52 kDa), 2 hr HPMA copolymer (26 kDa) and G5.0-OH; 6 hr and 24 hr G7.0-OH and n=3 for 1 wk HPMA copolymer (52 kDa). *** indicates a statistically significant difference, $p < 0.001$; ** $p < 0.01$.

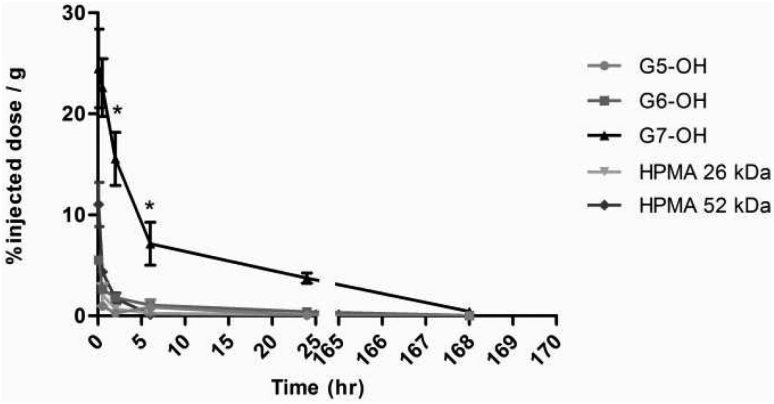

Figure 10A.

Percentage of injected dose / g of plasma tissue for PAMAM dendrimers and HPMA copolymers, Values are Mean +/- SEM; n=5; except n=4 for 5 min HPMA copolymer (52 kDa), 2 hr HPMA copolymer (26 kDa) and G5.0-OH; 6 hr and 24 hr G7.0-OH and n=3 for 1 wk HPMA copolymer (52 kDa). * indicates a statistically significant difference, $p < 0.05$.

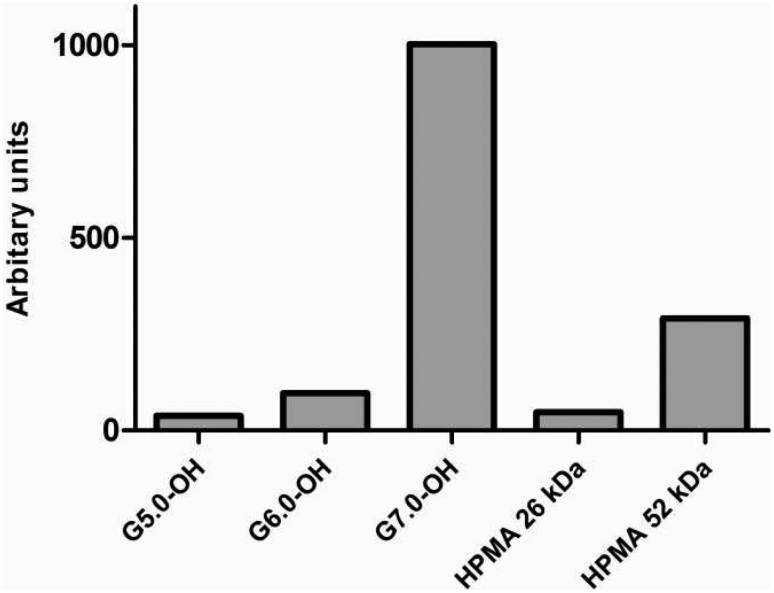

Figure 10B.
Area under the curve of plasma time course for PAMAM dendrimers and HPMA copolymers in percentage of injected radioactive dose.

Table 1

Composition of HPMA-based polymers

Monomer	**HPMA copolymer**		**HPMA copolymer**		**HPMA homopolymer**	
	Poly(HPMA-(GG-ONp)-(Tyr))		**Poly(HPMA-(GG-EtOH)-(Tyr))**		**Poly(HPMA-(Tyr))**	
	Feed mol %	***mmol / g of polymer***	***Feed mol %***	***mmol / g of polymer***	***Feed mol %***	***mmol / g of polymer***
MA-Tyr methyl ester	2	0.11 0.04[#]	2	0.12 0.22[#]	1	0.07
MA-GG-ethanolamine	0	0	20	1.2	0	0
MA-GG-ONP	20	1.1	0	0	0	0
HPMA	78	4.30	78	4.71	99	6.85

Numbers are theoretical values based on feed mole composition

[#]Measured values based on amino acid analysis

Biomacromolecules. Author manuscript; available in PMC 2012 October 19.

Table 2

Characterization of PAMAM dendrimers and HPMA copolymers

Polymer	G5.0-OH	G6.0-OH	G7.0-OH	HPMA copolymers	
Weight average molecular weight (kDa)	28.950 *	58.298 *	116.993 *	26.0 +/- 2.0	52.0 +/- 5.0
Number average molecular weight	ND	ND	ND	21.0+/- 3.6	27.0+/- 5.0
Poly dispersity Index	ND	ND	ND	1.3 +/- 0.2	1.9 +/- 0.2
Hydrodynamic radius (R_h) (nm)	2.3 +/- 0.2	3.0 +/- 0.2	4.0 +/- 0.1	1.4 +/- 0.0	3.3 +/- 0.2
Zeta Potential (mV)	1.69 +/- 0.21	2.28 +/- 0.48	-1.3 +/- 0.06	-14.66 +/- 0.83	-1.46 +/- 0.29
Number of surface hydroxyl groups	128 *	256 *	512 *	ND	ND

* Theoretical values based on perfect dendrimer synthesis47; Values are Mean +/- SD (n=3)